Geant4 simulations of monochromatic Cherenkov radiation in thin quartz targets for different experimental conditions

B Đurnić[1,2,3], A Potylitsyn[1], A Bogdanov[1] and S Gogolev[1]

[1] National Research Tomsk Polytechnic University (TPU), Lenin Avenue 30, Tomsk 634050, Russia

[2] Physics Department, Faculty of Sciences, University of Novi Sad, Novi Sad 21000, Serbia

Abstract: In light of our recent research, we discussed the possibility of observing quasi-monochromatic Cherenkov Radiation (ChR) spectral lines from a dispersive medium (thin quartz radiator). Such experimental results were verified on the Mainz Microtron MAMI, Germany [1], while both the polarization currents analytical model [2] and Geant4 [3] simulations were used to analyze the results. To describe the Cherenkov radiation process, the Geant4 toolkit uses only the approximation obtainable for an infinitely thick emitter ($\cos\theta = 1/\beta n(\lambda)$, where θ is Cherenkov's angle of emission, β is reduced velocity, and $n(\lambda)$ is a refractive index as a function of emitted radiation's wavelength λ) and doesn't consider its actual dimensions. Tamm's theory [4] predicts some broadening of the ChR angular distribution with a radiator thinning. Consequently, Geant4 gave inadequate results for the pencil-like electron beams compared to the polarization currents model and the experiment. However, unlike in the analytical calculations, we needed to consider more realistic Gaussian electron beams to obtain better results with Geant4. Therefore, obtained results primarily manifest beam characteristics rather than the ChR itself, i.e., its intrinsic characteristics are masked. Now, the idea is to present additional simulation results with further variations of the quartz's thickness (in preparation for future experiments), confirming the last conclusion without any doubt.

1. Introduction

The Cherenkov radiation (ChR) [5] process is widely known for its unique characteristics of detecting relativistic and ultrarelativistic charged particles. It's done via a continuous spectrum of emitted photons, ranging from sub-THz/THz [6] to "soft" X-ray regions [7]. For its characteristics are irreplaceable, nowadays, many detector systems [8], accelerator beam diagnostic systems [9], high-energy physics experiments [10], etc., are based on this radiation. Moreover, with the development of new materials, one got the possibility to obtain the ChR in some more exotic materials [11, 12].

According to experiments [13, 14] and the standard Tamm's theory [15], if a charged particle moves through a medium with a speed υ greater than the phase velocity of the light, ChR photons are emitted. In the case of an infinitely thick emitter, the photons are emitted along an infinitely thin cone, and relative to the direction of the relativistic particle, the angle of emission can be expressed as

$$\theta_{\mathrm{Ch}} = \arccos\left(\frac{1}{\beta \cdot n(\lambda)}\right). \quad (1)$$

[3] Corresponding author: zobla96@gmail.com

In the given equation, β is the relative velocity of the charged particle ($\beta = v/c$), while $n(\lambda)$ is the material's refractive index with the dependence of the emitted photon's wavelength λ. Such a dependence on the wavelength implies a dispersive emission of the ChR. According to the equation, the ChR generation condition can be written as

$$\beta \cdot n(\lambda) \geq 1. \tag{2}$$

Notably, the Geant4 toolkit uses exactly equation (1) in its simulations. However, as mentioned, equation (1) only describes an ideal case of an infinitely thick emitter, while in reality, the ChR cone has a specific thickness, given in Tamm's theory [4] as

$$\Delta\theta_{\mathrm{Ch}} \sim \frac{2\lambda}{\pi L \sin\theta_{\mathrm{Ch}}}, \tag{3}$$

where L is the length of the charged particle's trajectory (the thickness of the radiator, in our case, a thin plate). The broadening predicted in equation (3) is a consequence of the ChR wave nature and is observable unless the condition $\lambda \ll L$ is satisfied. In our previous analyses, we used another wave nature-based model to describe results – the polarization currents model [2, 16, 17]. For instance, that model gave good results compared to the experiment, even though pencil-like electron beams were considered [1].

Although the ChR is widely used, only recently was proposed and experimentally confirmed to detect it as quasi-monochromatic peaks [1] instead of the typical broad spectrum. To achieve that, one must use materials with frequency dependence, e.g., quartz, as in the given experiment. In order to extract ChR from a radiator bulk into a vacuum, one should tilt it as in figure 1. Therefore, considering the ChR cone part that leaves the plate and using Snell's law and equation (1), one can write

$$\theta_{\mathrm{vac}} = \psi + \arcsin\left[n(\lambda)\sin\left(\arccos\left(\frac{1}{\beta \cdot n(\lambda)}\right) - \psi\right)\right], \tag{4}$$

while the angles from the equation are provided in figure 1. After leaving the plate, ChR continues to propagate throughout the vacuum and preserves the original dispersion generated due to the quartz's function $n(\lambda)$ [18]. Therefore, after propagating a significant distance, the ChR gets resolved over various wavelengths, and by placing a small aperture detector, one can obtain quasi-monochromatic ChR peaks.

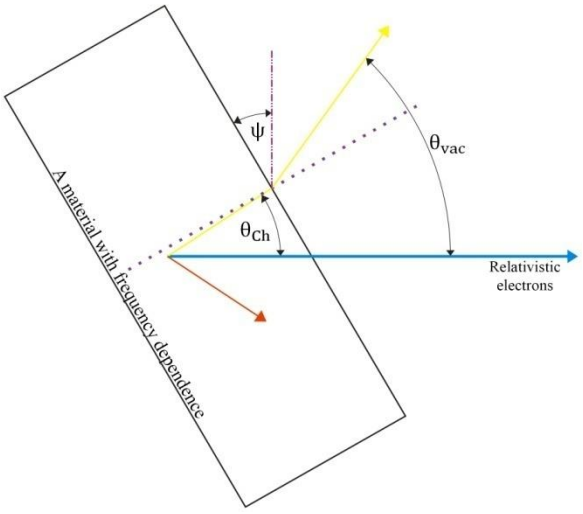

Figure 1 The propagation and characteristic angles of the Cherenkov radiation generated by relativistic electrons in an inclined material

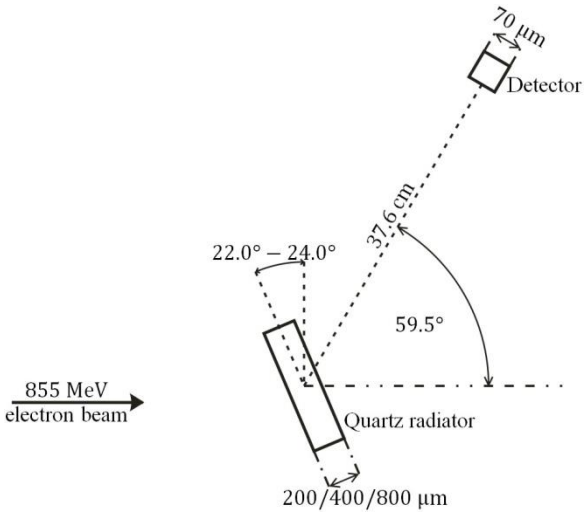

Figure 2 The scheme of the setup used in Geant4 simulations

Geant4 [3, 19] simulations were done using the experimental setup data [1], and we will shortly present those data here, starting with a scheme of the experiment in figure 2. Even though Geant4 was used (version 11.0.0), it's necessary to show the setup as a schematic view due to the specific ratios.

As shown in the figure, unlike in our previous analysis [20] where we considered only the experimental thickness, i.e., 200 μm, in this paper, we will consider three different thicknesses of the quartz radiator (200 μm, 400 μm, and 800 μm). Also, it should be pointed out that the results presented in this paper are the preparation for the future experiment that will be conducted due to the interest raised by the previous analysis of the 200 μm case.

We will consider the quartz radiator with experimental inclination angles between 22.0° and 24.0°. As we have explained in our previous analysis, unlike in the polarization currents model calculations, to obtain satisfactory results with Geant4, one should use a realistic, Gaussian shape profile of the electron beam, with the experimental value $\sigma = 536$ μm. This paper will confirm that by varying the radiator thickness and using simulation runs of 10 billion electrons. In our analysis, we neglected the beam divergence due to its small experimental value (14 μrad).

In Geant4 simulations, most of the results are obtained using G4EmStandardPhysics, which is, for experimental energies, based on the "WentzelVI" [21] electron multiple scattering model. On the other hand, G4EmStandardPhysics_option3 will be used to consider the "Urban" [22] electron multiple scattering model.

The obtained results will be presented over the two following sections, while the paper will be finished with a summary and discussion of the results.

2. Pencil-like electron beam results

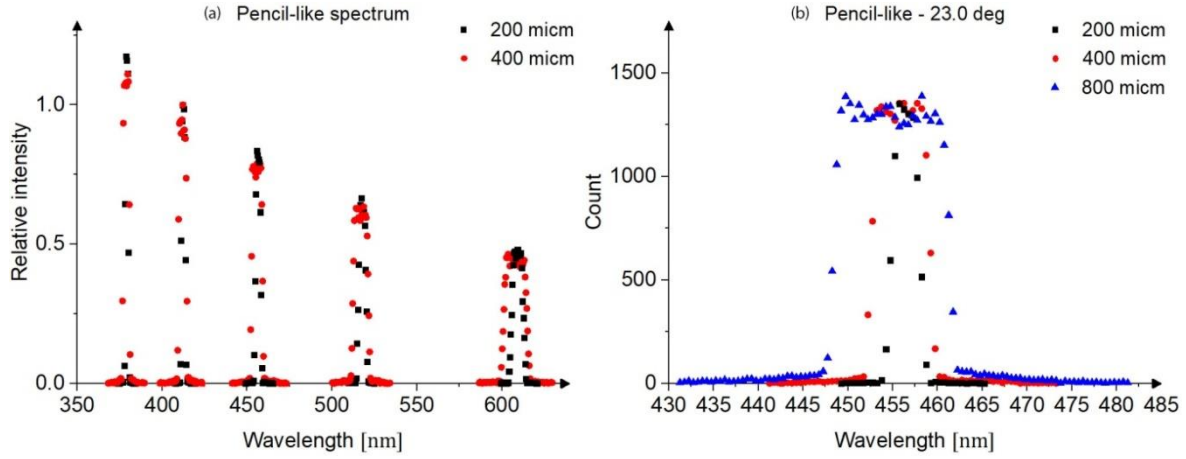

Figure 3 (a) The spectra comparison of quasi-monochromatic ChR peaks obtained for two radiator thicknesses using pencil-like electron beam profiles (b) The pencil-like peak obtained for the radiator inclination angle of 23.0° using various radiator widths

Figure 3 (a) compares a new whole spectrum of pencil-like peaks obtained using the radiator thickness of 400 μm with the previously obtained 200 μm spectrum. The figure shows that the new peaks have comparable intensities and spectral locations with the previously obtained peaks. Now, it would be interesting to zoom in on one of the peaks, e.g., the 23.0° peak as in figure 3 (b), and observe differences for a specific peak based on the radiator thickness. As the figure provides the actual count information, one can observe that the bin count changes only statistically around a constant value. However, the intensity of peaks changes significantly, i.e., as the radiator thickness increases, the peak gets wider and wider. In fact, as one doubles the radiator thickness, the intensity also gets doubled. The rule can be easily explained by paying attention to the ChR theory and the setup. As pointed out, depending on the location of the ChR emission, the photons must have different energies to be

detected. Moreover, the radiator's first and last layers are displaced with the thickness increase. Consequently, only photons with slightly changed energy can be detected from new layers.

Also, one can notice that the background of the peaks increases with the thickness, which could be attributed to the scattering effects. However, the detected ChR from electrons that didn't scatter is dominant as they already possess the proper direction for detecting ChR photons in the given geometry. Here, it should be pointed out that changing Geant4 "cut" values could significantly impact the shape of peaks. However, even as such, the upcoming results wouldn't be affected.

In our previous 200 μm thickness analysis [20], we considered the distribution of detected events and average wavelengths per detector bins. All the rules observed there could also be applied here with additional statistical changes. Therefore, in this paper, we won't consider detection distributions.

On the other hand, it would be interesting to consider another electron multiple scattering model for two radiator widths and see how it affects the peaks. Figure 4 (a) compares peaks obtained in different electron multiple scattering models using a 400 μm thickness radiator. The presented peaks have the same character as those obtained using 200 μm [20], and a question of an additional peak could be raised. Figure 4 (b) compares the different radiator thickness peaks obtained using the same Urban model. Unlike in figure 3 (b), the 400 μm peak doesn't have the doubled width but is slightly higher. However, in total, the intensity of the 400 μm peak is still doubled.

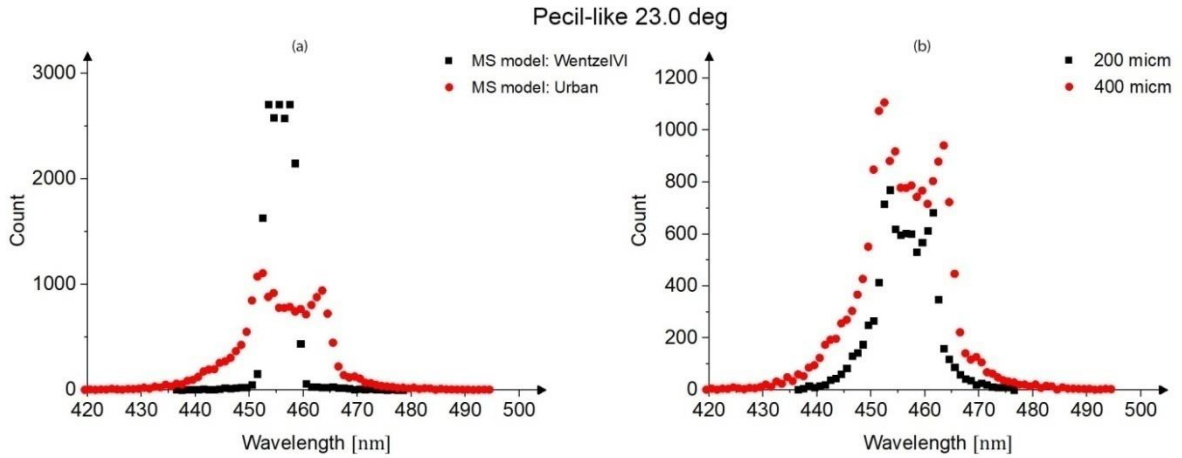

Figure 4 (a) The peaks obtained using a 400 μm thickness radiator and two Geant4 electron multiple scattering model (b) Comparison of peaks obtained using the Urban model and two radiator thicknesses

3. Gaussian electron beam results

Our previous analysis discussed that the Gaussian beam profile mostly masks the ChR characteristics in Geant4. Consequently, the results turned out much closer to the experimental ones, and we concluded that considering the beam profile for obtaining plausible data is essential. Now, after the previous section differences, if the masking effects are really present, we would expect meager differences between peaks in the Gaussian case.

For that purpose, let's consider the spectra of peaks in figure 5 obtained in the Gaussian electron beam profile case for two different radiator thicknesses. All the peaks are fitted with bi-Gaussian functions and normalized to the value of the 23.5° peak, as it was the highest-intensity experimental peak [1]. One can notice that both relative intensities and spectral locations of peaks are statistically comparable. However, our interest is to observe differences in a specific peak for various thicknesses.

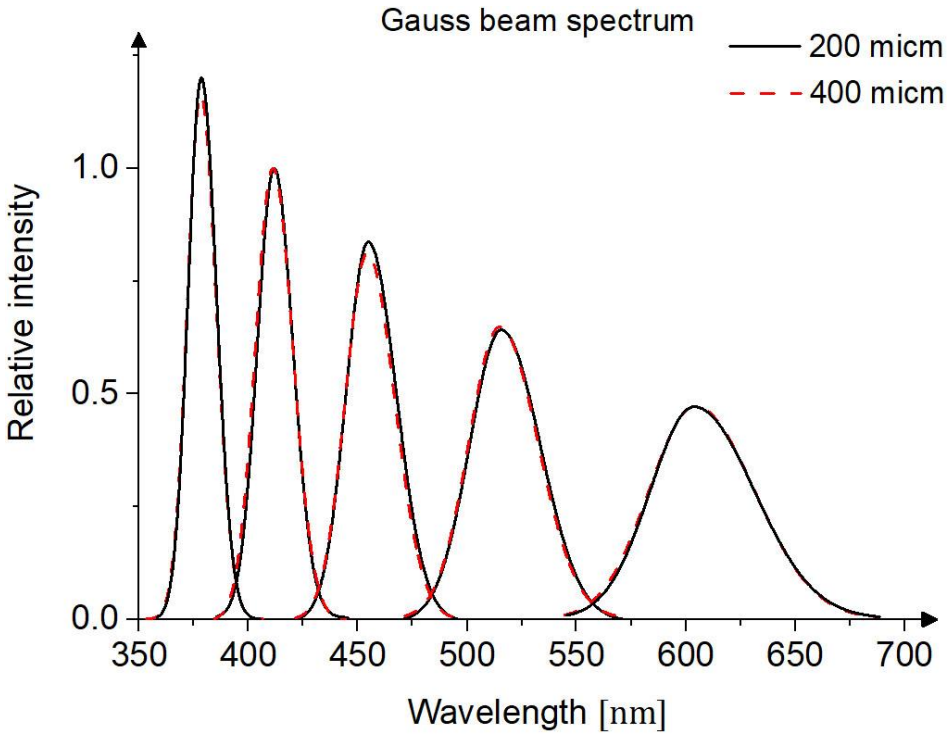

Figure 5 The spectra comparison of quasi-monochromatic ChR peaks obtained for two radiator thicknesses using Gaussian electron beam profiles

Figure 6 (a) provides the zoomed-in 23.0° peak of various radiator thicknesses with actual detection counts obtained in simulations. At first sight, one can make similar but opposite of the last section's observations, i.e., by increasing the thickness twice, the intensity also increases twice, but on the count of the peak's height, not width. The increase in the intensity comes as no big surprise as the distance of the charged particle in the radiator doubled, so it's evident that the number of steps doubled as well. However, unlike in figure 3, the width of peaks remains constant, which directly confirms our previous conclusion of beam profile masking effects. Moreover, we provide figure 6 (b) as a possibly better view of the peaks' differences (similarities). The figure shows the same data sets after fitting them with bi-Gaussian functions and normalizing them. It should be pointed out that even Geant4 "cut" values can't affect the peaks significantly due to the masking effects.

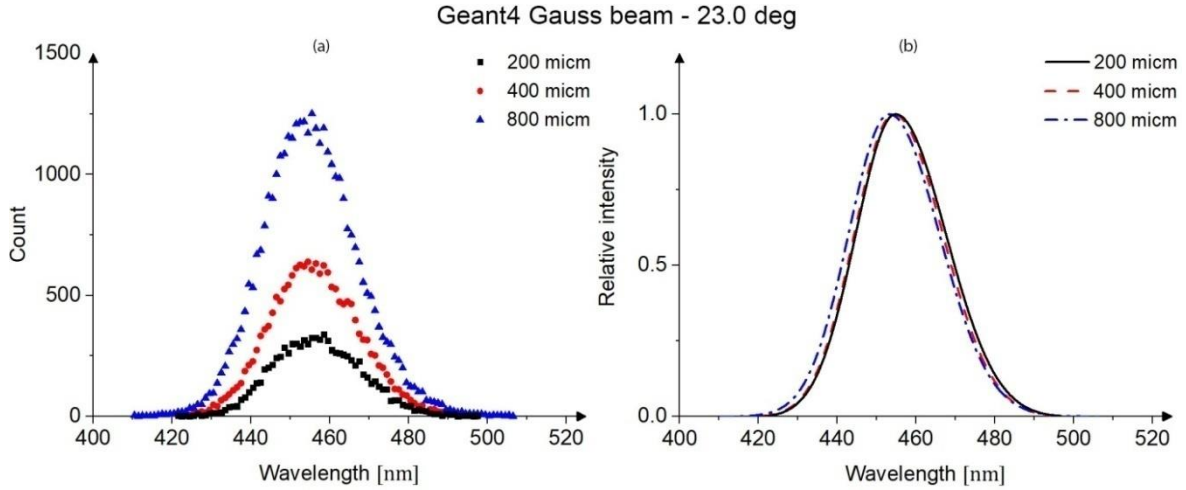

Figure 6 (a) The actual counts of 23.0° peaks obtained for various radiator thicknesses using Gaussian beam profile (b) The same peaks after fitting them with bi-Gaussian functions and normalizing them

Similar masking effects can be observed using the Gaussian beam profiles and the Urban electron multiple scattering model, shown in figure 7. Even though the differences in figure 4 are significant, one loses the information about a specific pencil-like beam due to the masking effects and gets a total picture of combined pencil-like beams of various intensities.

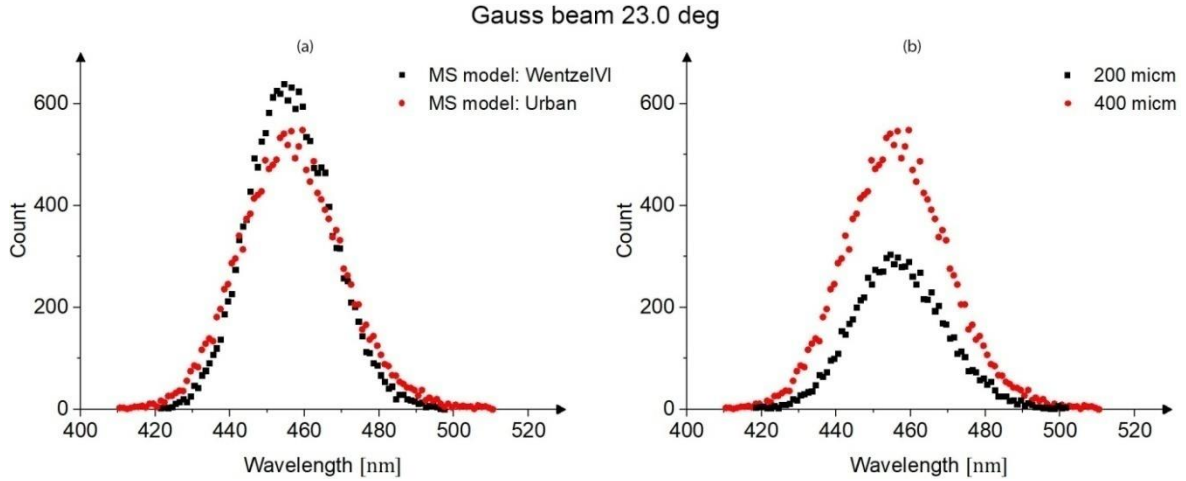

Figure 7 (a) Comparison of the peaks obtained using Gaussian beams, two different electron multiple scattering models, and the radiator of 400 μm thickness (b) Comparison of peaks obtained using the Urban model and two radiator thicknesses

4. Summary and discussion

In preparation for the future experiment and to confirm results previously obtained using the 200 μm thickness radiator, we consider various radiator thicknesses. The results and conclusions agree with the previous ones and show the importance of using the real electron beam profile alongside the wave nature of ChR while analyzing results.

In the pencil-like case, with the increase of the radiator's thickness, the peaks get wider, and their intensity increases, while the bin count remains statistically constant. However, Geant4 still gave inadequate results as peaks remained exceptionally narrow despite the widening.

On the contrary, when Gaussian beam profiles are used, the situation is opposite due to the masking effects. In this case, the intensity again increases with the radiator thickness, but on the count of the bins' intensities, while the peaks have a constant width. Besides the shape of the peaks, the spectrum of 400 μm radiator thickness peaks normalized to the angle of 23.5° preserves statistically the same intensities as in the 200 μm radiator thickness case. The same can be said about the peaks' spectral locations.

The detector efficiency wasn't included in the analysis yet. However, it's unimportant for this paper as the goal was to compare results obtained in Geant4 using various radiator thicknesses. Besides that, as shown in the previous analysis, the polarization currents analytical model gave results that better describe the experimental results than the Geant4 simulations, despite using pencil-like beams. Therefore, the previous conclusion that the theoretical model should be used alongside the beam characteristics remains valid and should be applied in the future.

5. References

[1] Potylitsyn A, Kube G, Novokshonov A, Vukolov A, Gogolev S, Alexeev B, Klag P and Lauth W 2021 *Phys. Lett.* A **417** 127680

[2] Karlovets D, Potylitsyn A 2009 *Phys. Lett.* A **373** 1988-96

[3] Agostinelli S *et al* 2003 *Nucl. Instr. Meth.* A **506** 250–303

[4] Tamm I E 1939 *J. of Phys. USSR* **1** 439–454

[5] Jelley J V 1958 *Cherenkov radiation and its Applications* (New York: Pergamon Press)

[6] Cook A M, Tikhoplav R, Tochitsky S Y, Travish G, Williams O B and Rosenzweig J B 2009 *Phys. Rev. Lett.* **103**(9) 095003

[7] Knulst W, Luiten O J, van der Wiel M J and Verhoeven J 2001 *Appl. Phys. Lett.* **79** 2999–3001

[8] Fukuda S 2003 *Nuc. Instr. and Meth. in Phys. Res.* A **501** 418–62

[9] Alves D *et al* 2019 *IBIC (Malmo)* THAO01 pp 660–4

[10] Avoni G *et al* 2018 *J. Inst.* **13** P07017

[11] Chang G, Chen LJ and Kärtner F X 2010 *Opt. Lett.* **35**(14) 2361-3

[12] Xi S, Chen H, Jiang T, Ran L, Haungfu J, Wu B I, Kong J A and Chen M 2009 *Phys. Rev. Lett.* 103 194801

[13] Cherenkov P A 1934 *Dokl. Akad. Nauk. USSR* **2**(8) 451–4 (in Russian)

[14] Vavilov S I 1934 *Dokl. Akad. Nauk. USSR* **2**(8) 457–9. (in Russian)

[15] Frank I M and Tamm I E 1937 *Dokl. Acad. Sci. USSR* **14** 109–14

[16] Potylitsyn A P and Gogolev S Yu 2019 *Phys. Part. Nucl. Lett.* **16**(2) 127–32

[17] Gogolev S Yu and Potylitsyn A P 2019 *Phys. Lett.* A **383**(9) 888–93

[18] Malitson I H 1965 *J. Opt. Soc. Am.* **55**(10) 1205–9

[19] Allison J *et al* 2016 *Nucl. Instr. Meth.* A **835** 186–225

[20] Đurnić B, Potylitsyn A and Bogdanov A. *Phys. Part. Nucl. Lett.* (in Press)

[21] Ivanchenko V N, Kadri O, Marie M and Urban L 2010 *J. Phys: Conference Series* **219** 032045

[22] Urbán L 2006 Technical Report, CERN, Geneva